RESEARCH PAPER

OncoImmunology 1:9, 1527–1536; December 2012; © 2012 Landes Bioscience

Cardiotrophin-1 determines liver engraftment of syngenic colon carcinoma cells through an immune system-mediated mechanism

Matilde Bustos,[1,†] Juan Dubrot,[1,†] Eduardo Martinez-Anso,[1] Eduardo Larequi,[1] David Castaño,[1] Asis Palazon,[1] Idoia Belza,[1] Miguel F. Sanmamed,[1,3] Jose Luis Perez-Gracia,[3] Carlos Ortiz de Solorzano,[2] Carlos Alfaro[1,‡] and Ignacio Melero[1,3,‡,*]

[1]Gene Therapy and Hepatology Unit; Center for Applied Medical Research; University Clinic of Navarra; Pamplona, Spain; [2]Cancer Imaging; Center for Applied Medical Research; University Clinic of Navarra; Pamplona, Spain; [3]Oncology Department; University Clinic of Navarra; Pamplona, Spain

[†]These authors contributed equally to this work.

[‡]These authors share equal credit for senior authorship.

Keywords: Cardiotrophin-1, intrahepatic lymphocytes, liver metastasis, tumor immunology

Cardiotrophin-1 (CT-1/CTF1) is a member of the interleukin-6 (IL-6) family of cytokines that stimulates STAT-3 phosphorylation in cells bearing the cognate receptor. We report that *Ctf1*$^{-/-}$ mice (hereby referred to as *CT-1*$^{-/-}$ mice) are resistant to the hepatic engraftment of MC38 colon carcinoma cells, while these cells engraft normally in the mouse subcutaneous tissue. Tumor intake in the liver could be enhanced by the systemic delivery of a recombinant adenovirus encoding CT-1, which also partly rescued the resistance of *CT-1*$^{-/-}$ mice to the hepatic engraftment of MC38 cells. Moreover, systemic treatment of wild-type (WT) mice with a novel antibody-neutralizing mouse CT-1 also reduced engraftment of this model. Conversely, experiments with Panc02 pancreatic cancer and B16-OVA melanoma cells in *CT-1*$^{-/-}$ mice revealed rates of hepatic engraftment similar to those observed in WT mice. The mechanism whereby CT-1 renders the liver permissive for MC38 metastasis involves T lymphocytes and natural killer (NK) cells, as shown by selective depletion experiments and in genetically deficient mice. However, no obvious changes in the number or cell killing capacity of liver lymphocytes in *CT-1*$^{-/-}$ animals could be substantiated. These findings demonstrate that the seed and soil concept to understand metastasis can be locally influenced by cytokines as well as by the cellular immune system.

Introduction

Cardiotrophin-1 (CT-1/CTF1) is a member of the interleukin (IL)-6 family of cytokines, which includes—besides IL-6 and CT -1—IL-11, IL-27, leukemia inhibitory factor (LIF), ciliary neurotrophic factor (CNTF), oncostatin M (OSM), cardiotrophin-like cytokine (CLC) and neuropoietin (NP). These cytokines are commonly referred to as glycoprotein 130 (gp130) ligands/cytokines since all of them utilize gp130 as a common subunit for signal transduction within their receptor complexes. Although there is some crosstalk among gp130 cytokines, there is no signal transduction cascade that is common to all family members. Thus, when CT-1 binds to the specific α receptor, it triggers its heterodimeric association with gp130 to form a signaling complex composed of the signal-transducing gp130Rβ and LIF receptor β (LIFRβ).[1] The engagement of gp130 by cytokine-specific α chains triggers the activation of three signaling cassettes, including the JAK-STAT pathway as well as a dual molecular cascade mediated by the cytoplasmic protein tyrosine phosphatase SHP2, which activates the Ras-ERK1/2 MAPK and PI3K/AKT pathways.[2] CT-1 was originally described to be specifically expressed in the heart is also expressed by many other tissues such as the skeletal muscle, kidneys, lungs and liver, where it exerts potent hepatoprotective effects.[3–6] In addition, an important role of CT-1 in glucose and lipid metabolism has recently been unraveled.[7] Nevertheless, CT-1-deficient mice are viable at birth and indistinguishable from their wild-type counterparts. Of note, CT-1 deficiency is associated with adult-onset obesity.[7]

Very little is known about the links between CT-1 and cancer. The trophic effects of this cytokine would suggest a pro-mitogenic activity on cancer cells, but there is no experimental evidence that supports this contention. Interestingly, cytokines of the IL-6 family can be used by cancer cells to adapt and survive to chemotherapeutic stress.[8] In addition, CT-1 is able to promote neo-angiogenesis during normal tissue regeneration and conceivably also in the tumor microenvironment.[9]

There is a conspicuous lack of knowledge regarding the effects of CT-1 on cells of the immune system, in spite of the wide expression of the receptor complex formed by gp130 and LIFR. Importantly, a significant body of work has been performed to

*Correspondence to: Ignacio Melero; Email: imelero@unav.es
Submitted: 07/27/12; Revised: 10/08/12; Accepted: 10/09/12
http://dx.doi.org/10.4161/onci.22504

characterize the role of the gp130 signaling cytokines during inflammation, suggesting that this receptor constitutes a prominent factor in balancing pro- and anti-inflammatory responses. Moreover, while there are studies suggesting that gp130-mediated signaling may be critical in oncogenesis, other reports demonstrate the ability of some gp130 family cytokines, such as OSM and IL-27, to block tumor progression.[2] It is important to emphasize that gp130-mediated signaling exerts a broad range of biological effects in cancer. The gp130-mediated activation of STAT3 by a cognate cytokine or upon somatic mutation of the receptor-encoding gene is oncogenic and contributes to disease progression in several models of cancer. Conversely, the overexpression of IL-27 has been shown to result in an increased clearance of multiple tumor type in mice, a phenomenon that was associated with enhanced antitumor $CD8^+$ T-cell and natural killer (NK)-cell responses.[10]

In this study, we found that the adenovirus-mediated delivery of CT-1 promotes the growth of MC38 colon carcinoma cells in the mouse liver, while the neutralization of CT-1 with a monoclonal antibody mitigates engraftment. Altogether, these results suggest that CT-1 may constitute a valuable therapeutic target. Moreover, CT-1-null mice rejected the engraftment of MC38 colon carcinoma cells, either as injected in the hepatic parenchyma or disseminating upon intrasplenic injection. This resistance was not observed in the subcutaneous tissue and was found to be dependent on T and NK cells. These findings opens a new field for the study of CT-1, whose mRNA is expressed at baseline levels in the healthy liver.[5]

Results

Lack of CT-1 results in the rejection of MC38 colon carcinomas engrafted in the mouse liver. MC38 cells are a colon carcinoma cell line that readily grows in the liver of C57BL/6 mice, both when injected directly into the hepatic parenchyma and when injected in the spleen to metastasize through the portal vein. To test whether endogenous CT-1 could play a role in the engraftment of MC38 colon carcinoma cells, the liver of CT-1-null (*Ctf1*$^{-/-}$, hereafter referred to as *CT-1*$^{-/-}$) and wild-type (WT) mice was inoculated with tumor cells. As shown in **Figure 1A**, five out of seven *CT-1*$^{-/-}$ mice backcrossed into C57BL/6 background for ten generations rejected tumor cells, while in WT C57BL/6 and *Il6*$^{-/-}$ mice, engrafted cells gave rise to lethal liver tumors in three-four weeks. In order to completely exclude alloreactive rejection mechanisms, animals were further backcrossed to C57BL/6 for two additional generations selecting for the most C57BL/6 background-matched breeders by analyses of microsatellite polymorphism. Similar results were observed again with six out of eight *CT-1*$^{-/-}$ mice, completely rejecting tumors that readily grew in littermate controls hosted in the same cages (**Fig. 1B**). CT-SCAN images performed on day 14 after tumor-cell inoculation show an example of each type of mice, with a 3D computer-assisted reconstruction indicating the presence of early progressing liver metastases (**Fig. 1C**). Interestingly, WT, *CT-1*$^{-/-}$ and *Il6*$^{-/-}$ mice challenged with the same, lethal dose of MC38 cells in the subcutaneous tissue all developed rapidly progressing lethal tumors.

The resistance to the hepatic engraftment of tumor cells exhibited by *CT-1*$^{-/-}$ mice was related to the MC38 cell line, as we could not observe a similar phenotype when B16-OVA (melanoma) and Panc02 (pancreatic carcinoma) cells, representing to tumor types that are naturally prone to hepatic metastasis, were used (**Fig. S1**).

Interestingly, when *CT-1*$^{-/-}$ mice that had rejected an intrahepatic injection of MC38 cells were rechallenged in the dermis, eight out of ten mice did not develop tumors, while these cells readily engrafted in the subcutaneous tissue of *CT-1*$^{-/-}$ tumor-naïve animals as well as in WT mice (**Fig. 2**). These findings suggest the development of some type of immunological memory or vaccine-like effect following the first exposure of *CT-1*$^{-/-}$ livers to tumor cells.

The adenoviral delivery of CT-1 promotes hepatic engraftment of MC38 cell-derived tumors. To further explore the role of CT-1 in the progression of metastasis, we used a liver-targeting gene transfer approach based on a first-generation recombinant adenovirus encoding CT-1 (AdCT-1).[3] AdCT-1 was administered 48h before the hepatic inoculation of MC38 tumor cells. Our data show that AdCT-1 significantly enhances the engraftment and growth of tumor cells at day 14 following inoculation as compared with a LacZ-coding adenovirus AdLacZ = used as a control condition. Photographs of the abdomen of WT euthanized mice (**Fig. 3A**) show two examples per condition of hepatic tumor engraftment. Moreover, AdCT-1 given 2 d before the inoculation of tumor cells was able to partly rescue the resistance to engraftment of *CT-1*$^{-/-}$ mice (**Fig. 3B**). Hence, CT-1 gene transfer gave rise to progressing MC38 tumors in the liver of *CT-1*$^{-/-}$ mice.

At this point, we wondered whether CT-1 would constitute a necessary trophic factor for the hepatic growth of MC38 tumor cells. However, experiments performed in vitro showed that MC38 cells proliferate equally in the presence and in the absence of CT-1 (**Fig. S2A**). Of note, neutralizing CT-1 with a specific monoclonal antibody did not change the proliferation rate of cultured MC38 tumor cells (**Fig. S2B**).

Anti-CT-1 antibodies mitigate the progression of MC38 cell-derived liver metastasis. In order to explore the potential of CT-1 as a therapeutic target, we generated CT-1-specific monoclonal antibodies in *CT-1*$^{-/-}$ null mice. The MAB19 antibody was selected as it efficiently bound to both mouse and rat CT-1 in ELISA assays (**Fig. 4A**). MAB19 was neutralizing, since it partly inhibited the phosphorylation of STAT3 as induced by a short pulse (30 min) of CT-1 in mouse hepatocarcinoma Hepa 1–6 cells that had previously depleted from serum and growth factors overnight. Thus, MAB19 can neutralize the direct effects of recombinant CT-1, albeit not completely in these assays, as revealed by immunoblotting for the phosphorylated form of STAT3 (P-STAT3) (**Fig. 4B**).

Next, we intraperitoneally administered MAB19 to mice on days -3, -1, 1, 3 and 6 (day = hepatic injection of MC38 cells). As can be seen in **Figure 5A**, WT mice receiving MAB19 but not animals treated with a control antibody manifested a delay in the growth of liver MC38 cell-derived metastases, as assessed by surgical examination performed on day 14. Such an effect was

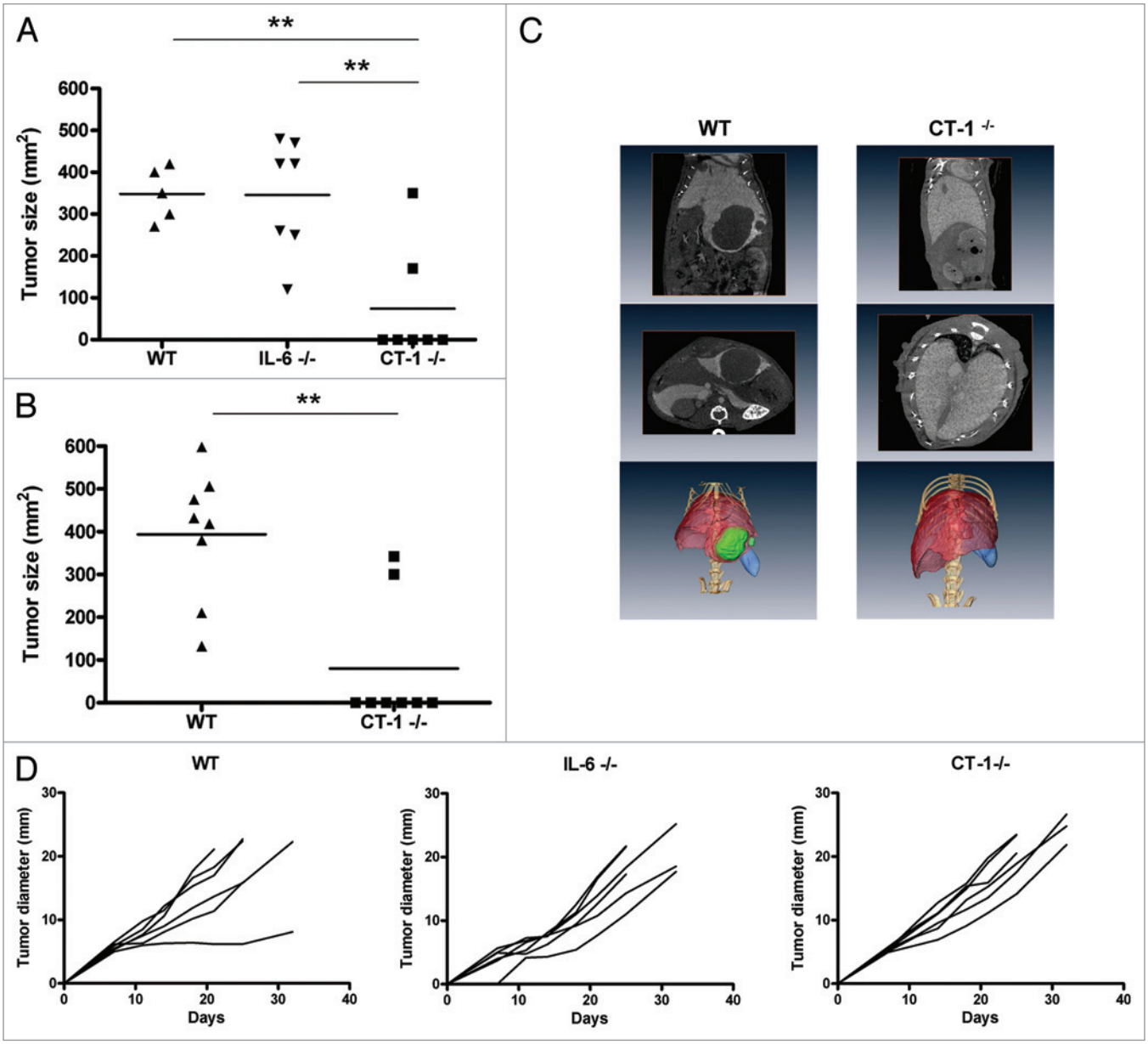

Figure 1. *CT-1*$^{-/-}$ mice are protected against the hepatic engraftment of MC38 colon cancer cells. (**A**) Individual size of MC38-derived tumors grafted in the liver for 14 d in wild type (WT), *Il6*$^{-/-}$ and CT-1$^{-/-}$ C57BL/6 mice. Mice were inoculated with 5×10^5 MC38 colon carcinoma cells in the surgically exposed left lobe of the liver. Liver tumors were measured 14 d after tumor cell inoculation (**$p < 0.01$). (**B**) Experiment as in (**A**), showing the size of liver tumors in WT and *CT-1*$^{-/-}$ mice backcrossed for two additional generations with selection for the most matched breeders by analyses of microsatellite polymorphism. (**C**) MicroCT images taken from representative mice per group on day 14 prior to surgery. (**D**) Littermate groups of mice of those shown in (A) were inoculated subcutaneously in the flank with 5×10^6 MC38 cells. A sequential individual follow-up of the tumor mean diameter is shown.

not observed in mice devoid of T, B and NK lymphocytes (*Rag2*$^{-/-}$ *Il2r*$\gamma^{-/-}$ mice), as shown in **Figure 5B**. In addition, MAB19, by virtue of its anti-CT-1 effects, extended post-surgery survival of mice receiving an intrahepatic inoculation of MC38 cells (**Fig. 5C**). Altogether, these findings indicate that the anti-tumorigenic effect of anti-CT-1 antibodies involves the immune system.

Hepatic engraftment of MC38 cells via the portal vein is also influenced by CT-1. When mice were injected intrasplenically with MC38 tumor cells, a model of intense metastatic dissemination through the portal vein, much smaller and a lower number of tumor nodules were observed *CT-1*$^{-/-}$ animals than in their WT counterparts. **Figure 6A** shows a histological image of representative tumor nodules, while **Figure 6B** shows quantitative analyses of tumor area in multiple non-serial liver slides stained with hematoxylin and eosin, which were consistent with the inspection of formalin-fixed organs. These data confirm that *CT-1*$^{-/-}$ livers are less prone to accept MC38 cell-derived metastatic emboli incoming from the spleen via the portal circulation than WT organs.

Involvement of the immune system in the pro-engraftment effects of CT-1. In order to study the potential involvement of

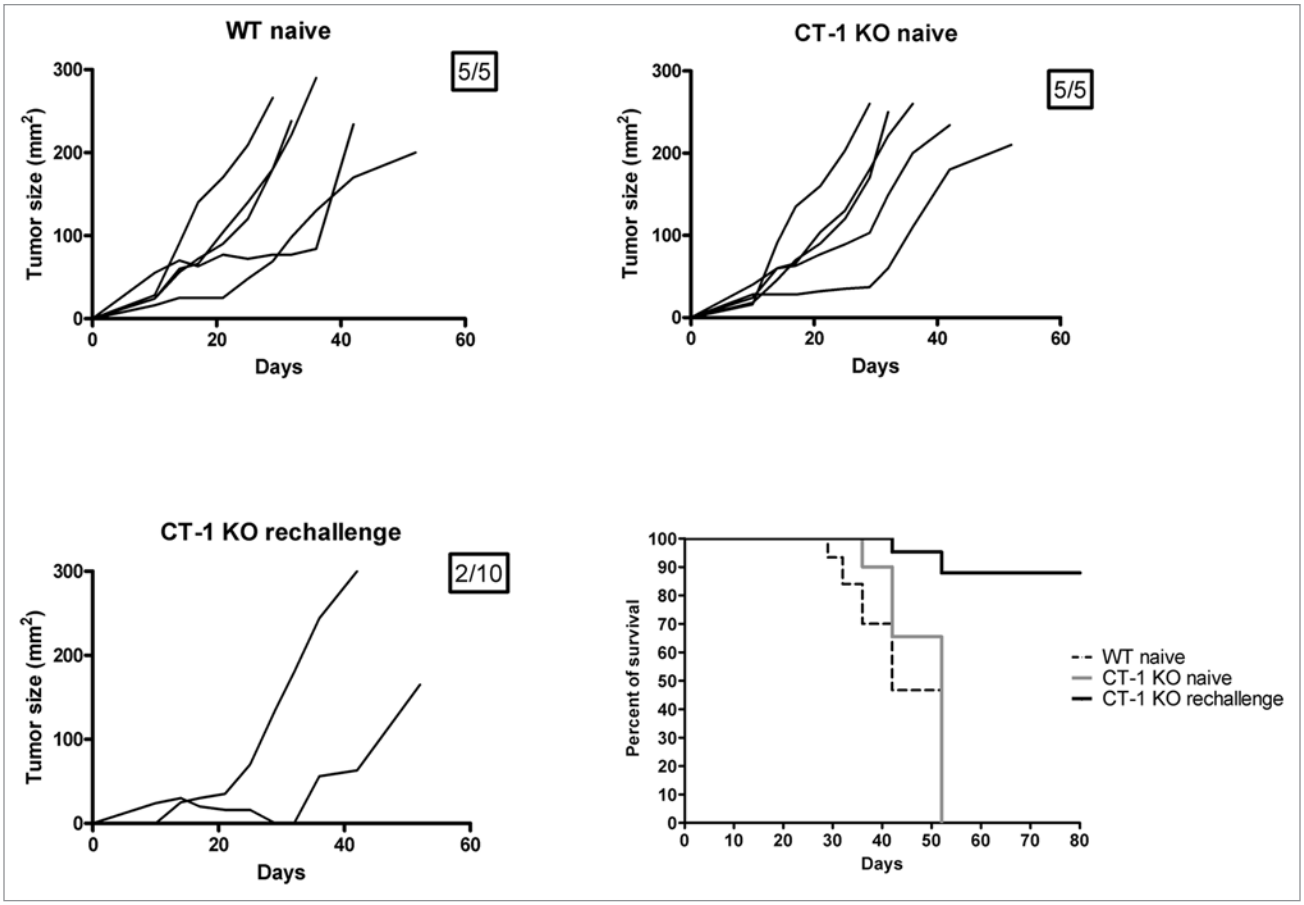

Figure 2. *CT-1*$^{-/-}$ mice rejecting intrahepatic MC38 cells become immune to a subcutaneous re-challenge with the same cells. Sequential size follow-up of subcutaneous tumors in mice inoculated with MC38 tumors in the dermis of tumor-naïve wild type (WT) mice, tumor-naïve *CT-1*$^{-/-}$ mice and *CT-1*$^{-/-}$ mice that had rejected a previous MC38 tumor challenge in the liver 3 mo before the subcutaneous challenge. A survival graph of the groups is included and the fraction of mice exhibiting terminal tumors is included in each graph.

the immune system in the observed phenotype, we selectively depleted (by means of specific monoclonal antibodies) T-cell subsets and NK cells. **Figure 7A** shows experiments performed by inoculating MC38 cells in the spleen and using the surface fraction of the liver covered with tumors, on day 14, as a readout. In line with previous observations, the area of *CT-1*$^{-/-}$ livers covered with tumor cells was lower than that of WT organs. Interestingly, the depletion of CD4$^+$ plus CD8$^+$ cells as well as of NK cells (with an anti-asialo GM1 antibody), resulted in a massive tumor progression in most instances. Indeed, the dual depletion of NK and T cells exerted the most dramatic effect, with some livers that were completely covered by tumor lesions at sacrifice. Next, these experiments were performed following the direct intrahepatic inoculation of tumor cells and using the size of the tumor nodules on day 14 as a readout. Results shown in **Figure 7B** render are comparable to those obtained with the portal vein dissemination model and indicate that T cells and NK cells (in this case depleted with an anti-NK1.1 monoclonal antibody) are involved in the resistance of *CT-1*$^{-/-}$ mice to the hepatic engraftment of MC38 tumor cells.

This being said, the intrahepatic percentage and absolute number of CD4$^+$ and CD8$^+$ T cells as well as of NK cells were similar results in *CT-1*$^{-/-}$ and WT mice (**Fig. S3**). Moreover, mononuclear leukocytes purified from the liver of *CT-1*$^{-/-}$ and WT mice, did not differ in their ability to kill MC38 and YAC-1 target cells, neither in baseline conditions nor when their cytolytic activity was boosted by the treatment of mice with polyI:C, indicating no obvious alterations in the cytolitic functions of intrahepatic *CT-1*$^{-/-}$ vs. WT immune cells (**Fig. S4**).

A possible clue to clarify these observations may come from the differential response of *CT-1*$^{-/-}$ mice to the hepatic engraftment of MC38, Panc02 and B16-OVA cells. Indeed, MHC Class I (H-2K^b and D^b) was robustly expressed on cultured MC38 cells, but not on Panc02 (weak expression) and B16-OVA (no expression) cells. However it could be induced by IFN-γ in every case (**Fig. S5**). One additional element in this setting could be represented by the ability of tumor cells to produce CT-1 themselves. To clarify this aspect, culture supernatants from the abovementioned cell lines were assayed for CT-1 content by ELISA. We found that all three cell lines secrete CT-1, although MC38 does so to much higher values, particularly when cultured in the presence of fetal bovine serum (**Fig. S6A**). The amount of secreted CT-1 correlates was found to correlate with *CT-1* mRNA expression levels as assessed by quantitative RT-PCR (**Fig. S6B**).

Although we observed an involvement of lymphocytes, we could not detect gross differences in the number or function of hepatic lymphocytes in WT vs. *CT-1*$^{-/-}$ mice. Hence, the observed discrepancies may be explained by a mechanism that depend on the local innate response against incoming MC38 tumor cells, followed by a T cell-mediated adaptive response. Irrespective of this hitherto unclear aspect, our data unravel a previously unknown effect of CT-1 in determining the hepatic permissiveness to metastatic colonization by colorectal cancer cells.

Discussion

The metastatic colonization of the liver is a common and often fatal outcome of colorectal cancer.[11,12] In the same setting, an abundant infiltration of the tumor mass with antigen-experienced CD8$^+$ T cells as well as elevated levels of chemotactic chemokines correlate with improved prognosis independent of multiple additional factors.[13,14] NK cells among the tumor infiltrate are also a favorable finding.[15] In this study, we report the surprising observation that *CT-1*$^{-/-}$ mice are resistant to liver engraftment by MC38 colorectal carcinoma cells. This effect was initially attributed to a putative activity of CT-1 on tumor cells, since CT-1 could—at least theoretically—operate as an anti-apoptotic or trophic factor. However, we observed that the exogenous administration of CT-1 to MC38 cells does not increase proliferation and that CT-1 neutralization with specific monoclonal antibody appears not to affect MC38 cell cultures. Therefore, the effects of CT-1 on liver engraftment turned out to be indirect and to pertain the liver as a soil for the metastatic seed.[16]

We have previously observed that healthy livers exhibit baseline expression levels of the CT-1-coding mRNA,[5] hence being "ready" to receive metastatic cells. Cirrhotic livers produce less CT-1 than their healthy counterparts (unpublished observations), and it is known that cirrhotic livers are comparatively less prone to undergo metastatic colonization.[17,18] Conversely, Okuno and colleagues[19] demonstrated that the activation of the innate immune system with recombinant cytokines may prevent hepatic metastasis. Taken together, these findings suggest that the activation of innate immune effectors within the liver might inhibit metastatic colonization. Hence, local factors that repress innate antitumor responses would facilitate the hepatic engraftment of metastases. It should be noted that cytokines and their receptors constitute a very complex signaling system, implying that we may be ignoring key factors to interpret these results. For instance, it has been reported that tumor cells can release soluble forms of the gp130 receptor component that is shared by IL-6 and CT-1. The cytokine and its receptor act in solution as a molecular complex with modified functional properties.[20,21] The role of these molecular interplays will need to be addressed in subsequent investigations.

In addition to results obtained with knockout mice, genetic evidence for a critical role of CT-1 in the hepatic engraftment of colorectal carcinoma cells was provided by the transfer of a CT-1 expression cassette encoded by a recombinant adenovirus that infects most hepatocytes when given intravenously.[3,4] Gene transfer not only enhanced tumor growth in WT mice, but also rescued part of the resistance to MC38 cell-derived liver metastases of *CT-1*$^{-/-}$ mice. The recombinant adenovirus was given two days before tumor inoculation in order to precondition the soil to receive incoming tumor cells. Curiously, we could not obtain similar results with other tumors syngenic to C57BL/6 mice and known to generate hepatic metastases. The proportion of tumors that are sensitive to the effects of CT-1 remains to be determined, and at present it cannot be excluded that this may be a selective feature of colon cancer or even a peculiarity of MC38 cells. In this regard, a thorough examination of further C57BL/6-transplantable tumors, including sarcomas and lymphomas, is ongoing.

Another peculiar observation was that the subcutaneous tissue of *CT-1*$^{-/-}$ mice is perfectly permissive for the engraftment of

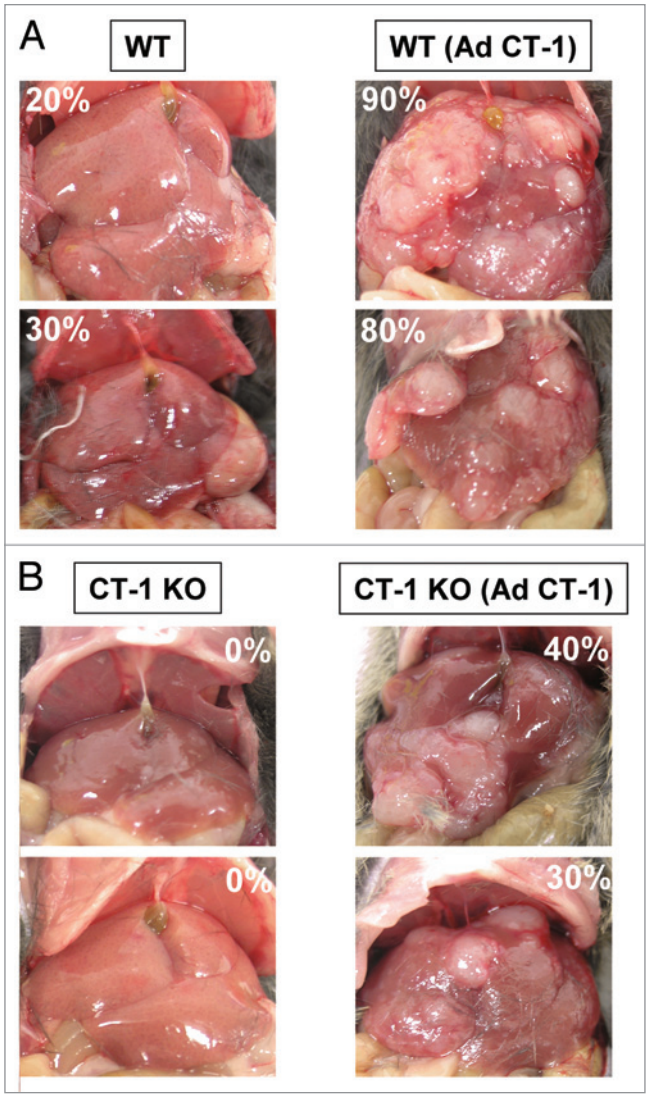

Figure 3. Adenoviral delivery of CT-1 to the liver promotes the growth of MC38 cell-derived hepatic metastasis. (**A and B**) AdCT-1 was intravenously injected two days before the intrahepatic administration of 5×10^6 MC38 tumor cells. Experiments were performed in wild type (WT) (**A**) or *CT-1*$^{-/-}$ (**B**) mice. Photographs of the dissected abdomen represent tumor progression at day 14. Percentages represent area of tumor referred to total liver surface, containing 100 pixels (4.2 mm × 5 mm) in each picture.

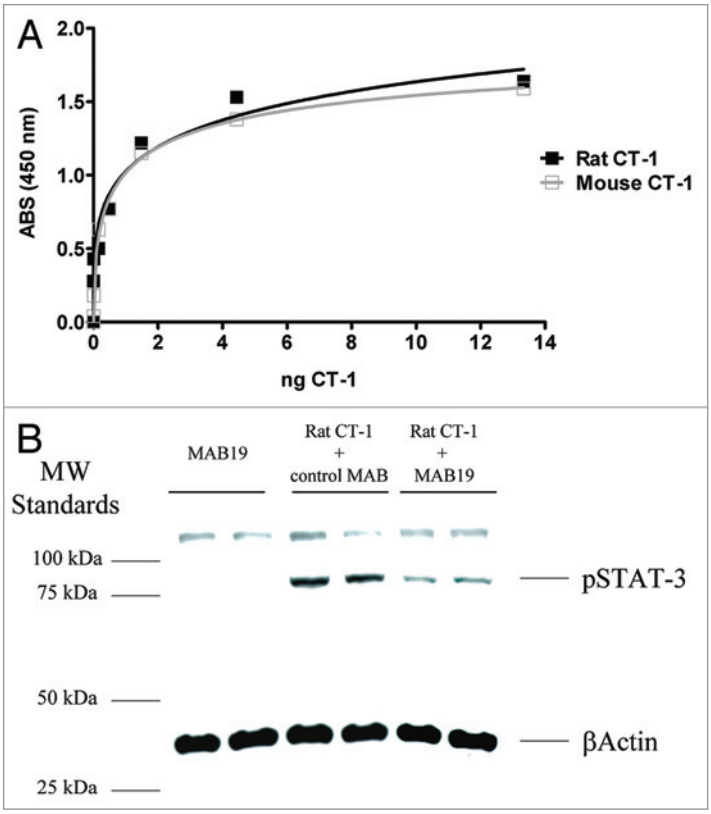

Figure 4. Generation of a neutralizing anti-CT-1 monoclonal antibody. (**A**) ELISA assays with recombinant mouse (gray) or rat (black) CT-1 adsorbed onto 96 wells plates. Plates were coated with 100 ng of recombinant CT-1 per well and several dilutions of the MAB19 monoclonal antibody were added. Specific signal was detected with a peroxidase-conjugated goat anti-mouse IgG (H^+L) and developed with TMB. (**B**) In vitro neutralization of recombinant rat CT-1 with MAB19 in Hepa 1–6 cells. Phosphorylation of STAT3 was measured by immunoblotting in cells stimulated with 2.5 ng/mL of rCT-1 after pre-incubation with 1 μg/mL of MAB19 or control antibodies. Equal sample load was controlled reanalyzing the stripped blots with an anti-β actin antibody.

MC38 cells. This might be related to differential baseline levels of CT-1 in the dermis and the liver. Additional explanation for this observation may be linked to the high density of immune cells in the liver.[22]

To study the therapeutic potential of our findings, we have developed a CT-1-neutralizing monoclonal antibody. This was a difficult task, mostly owing to the near identical sequence of CT-1 across species. To circumvent this issue, the antibody MAB19 was generated by immunizing *CT-1*$^{-/-}$ mice. Therefore, MAB19 constitutes an interesting tool for future investigational and perhaps therapeutic applications. The neutralizing effects of MAB19 were statistically significant but not meaningful enough from a survival perspective. It is quite possible that the levels of neutralization achieved were not sufficient to mimic the total lack of CT-1 that characterize *CT-1*$^{-/-}$ mice. Alternatively, prolonged periods of neutralization prior to the inoculation of tumor cells might be needed to properly pre-condition the target tissue. We are currently unable to explain the differential behavior of MC38, Panc02 and B16-OVA cell lines in molecular terms, though we have ruled out gross differences in their ability to produce CT-1 at the mRNA and protein levels.

The involvement of the immune system in the observed phenomena was suggested by two lines of evidence: (1) mice that rejected MC38 cell-derived hepatic metastases because of the lack of CT-1 become immune to a subcutaneous challenge with the same tumor cells and (2) the depletion or genetic ablation of T and NK cells neutralized the resistance of *CT-1*$^{-/-}$ mice to the metastatic colonization of their livers by MC38 cells. However, no obvious alterations in the abundance and cytolytic activity of hepatic and splenic immune cells could be substantiated in *CT-1*$^{-/-}$ mice.

Hence, it is possible that the events leading to tumor rejection are elicited locally upon the arrival of tumor cells but do not affect the bulk of hepatic lymphocytes. Our working model is that NK cells and T cells, operating as the main effectors of rejection, could be activated by a number of cytokines (including IFNα/β, IL-2, IL-12p70 and IL-18). The composition of such cytokine milieu would be different in the presence or in the absence of CT-1, hence specifically impacting how NK cells recognize and kill target cells. In this regard, it is known that CT-1 induces STAT3 activation in lymphocytes and tumor cells. It is possible that NK cells and T cells might be turned off by STAT3 activation.[23,24] Moreover, even if we did not observe any effect of CT-1 on the viability of cultured MC38 cells, the absence of CT-1 in vivo might result in some extent of, possibly immunogenic, tumor cell death.[25] No evidence is available yet to support or discard these contentions. The central hypothesis raised by this study is that CT-1 would act by weakening the hepatic immune system, hence accounting for an increased propensity of the liver to accept metastatic colonization, at least from specific carcinomas.

Further research is needed to determine the entire range of biological effects of CT-1 and the ability of this cytokine to influence immunity and inflammation in many different settings, including cancer immunotherapy.

Materials and Methods

Mice. *CT-1*$^{-/-}$ mice (provided by Dr. Pennica, Genentech) were backcrossed into a C57BL/6 background for 11 generations. The CT-1 genotype was confirmed in the breeders by genomic DNA isolation and polymerase chain reaction as previously described.[26] *Il6*$^{-/-}$ mice and C57BL/6 mice were originally obtained from The Jackson Laboratory (Bar Harbor) and bred in our animal facility. When indicated, *CT-1*$^{-/-}$ breeders were selected for microsatellite matching with C57BL/6 pure backgrounds (Bionostra). *Rag2*$^{-/-}$ *Il2rγ*$^{-/-}$ mice were obtained from The Jackson Laboratory and were bred in our animal facility under pathogen-free conditions. Mice that were obtained from The Jackson Laboratory were used between 6 and 14 weeks of age. Animal experiments were performed in accordance with Spanish laws and approval was obtained from the animal experimentation committee of the University of Navarra (Study 034/10 approval).

Tumor experiments. MC38, B16-OVA and Panc02 carcinoma cells have been previously described.[27–29] Cells are grown

in RPMI 1640 with Glutamax-I (Gibco Invitrogen, 61870–010) containing 10% heat-inactivated FBS (Sigma-Aldrich, 15F7524), 100 IU/mL penicillin and 100 mg/mL streptomycin (Biowhittaker, 17–603E). Cells were serially passaged when subconfluent as needed. Cells stocks were monitored to be mycoplasma free and have been validated for identity (RADIL; Case 6592–2012).

Mice were injected with the 5×10^6 MC38, 1×10^6 B16-OVA or 5×10^6 Panc02 cells to induce subcutaneous or hepatic tumors. When indicated, mice were injected intrasplenically with MC38 tumor cells to mimic portal vein dissemination. Fourteen days later, a laparotomy was performed and tumor nodules on the surface of the liver lobes were quantified.

Selective depletion of lymphocytes. A total of 200 μg per dose of CD4 and CD8-depleting monoclonal antibodies was administered i.p. to deplete different T-cell subpopulations. Anti-CD4 and anti-CD8β mAb were injected every other day for four times beginning 3 d before tumor injection, and then every 5th day. NK cell depletion was performed using anti-asialo GM1 (Wako Fine Chemicals, 986–10001) or anti-NK1.1 antibodies. A total of 20 μL of anti-asialo GM1 antibody or anti-NK1.1 antibody diluted with 180 μL of sterile saline was injected 2 d before tumor inoculation and every 3 d thereafter for a total of 5 doses.

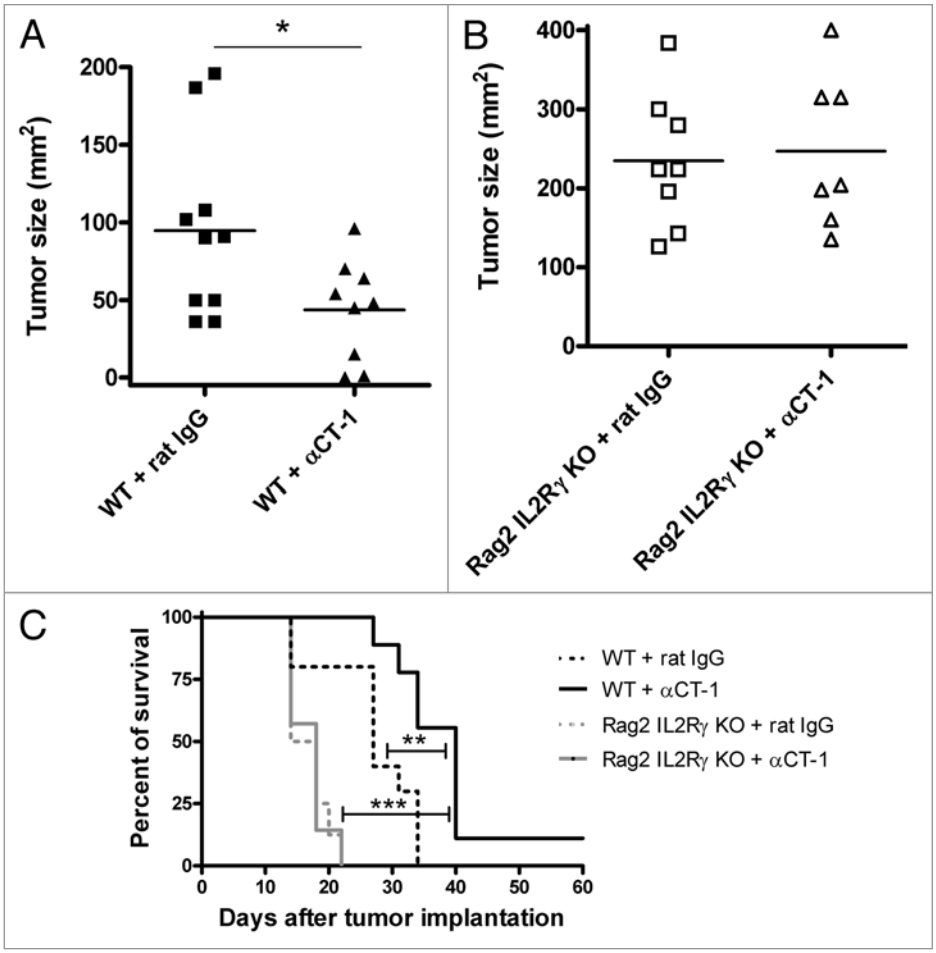

Figure 5. A neutralizing anti-CT-1 antibody decreases the growth of intrahepatic MC38 cells and prolongs survival. (**A and B**) Hepatic tumor sizes of wild type (WT) (**A**) or immunodeficient *Rag2*$^{-/-}$ *Il2rγ*$^{-/-}$ (**B**) mice challenged with 5×10^5 MC38 cells directly into the left lobe of the liver. Where indicated, mice were injected with 200 μg of the MAB19 on days -3, -1, 1, 3 and 6 after tumor inoculation or with irrelevant polyclonal rat Ig as a control. Tumors were measured on day 14 exposing the liver under anesthesia and mice were recovered from surgery (*$p < 0.05$). (**C**) Survival follow-up and log rank test comparisons (**$p < 0.01$; ***$p < 0.001$).

FACS analysis. FITC and PE-labeled antibodies specific for CD3, CD4, CD8, NK1.1, CD69, CD137, H-2K^b and H-2D^b markers (BD Bioscience) were used to characterize cell surface expression by multicolor flow cytometry. Cells (10^5) were washed in cold PBS and incubated for 15 min at 4°C with specific FITC or PE-labeled antibodies. For the analysis of surface MHC Class I expression, 10^3 UI/mL IFNγ was added for 48 h.

Quantitative RT-PCR for CT-1. Total cellular RNA was extracted with Trizol (Invitrogen, 12183–555) according to the protocol provided by the manufacturer. First-strand cDNA was synthesized from 1 μg total cellular RNA using an RNA PCR kit (Takara Bio Inc., RR019A) with random primers. Thereafter, cDNA was amplified using 30 and 28 cycles for CT-1 and β-actin, respectively. The following specific primers were used: CT-1, FWD 5'- AGC ATG AGC CAG AGG GAG GGA A -3' and REV 5'- TAT GCA GAC CAA TTG CTG GAG GAA-3'; β actin, FWD 5'-GTG GGG CGC CCC AGG CAC CA-3' and REV 5'-CTC CTT AAT GTC ACG CAC GAT TTC-3'. The thermocycling conditions for the targets were as follows: denaturing at 94°C for 30 sec, annealing at 60°C for 30 sec and extension at 72°C for 90 sec. Reactions were run on a QX100 Droplet Digital PCR System (Bio-Rad Laboratories, 186–3001). β actin was employed to normalize the amount of RNA used in each reaction. The amount of each transcript was expressed as the n-fold difference relative to the control transcript coding for β actin ($2^{\Delta Ct}$, where ΔCt represents the difference in threshold cycle between the control and target gene).

ELISA. ELISA for the detection of CT-1 was performed in supernatants from cell (MC38, Panc02 and B16-OVA) cultures, as previously described.[3]

Cytotoxicity assays. Cytotoxic activity against MC38 and YAC-1 cells was measured by the standard 5 h sodium chromate [^{51}Cr] release assay. One million target cells were labeled with 50 μCi [^{51}Cr] (PerkinElmer, NEZ020005MC) for 1 h at 37°C, washed and resuspended in RPMI 1640 (Gibco Invitrogen) containing 10% FBS from Sigma-Aldrich. Liver mononuclear

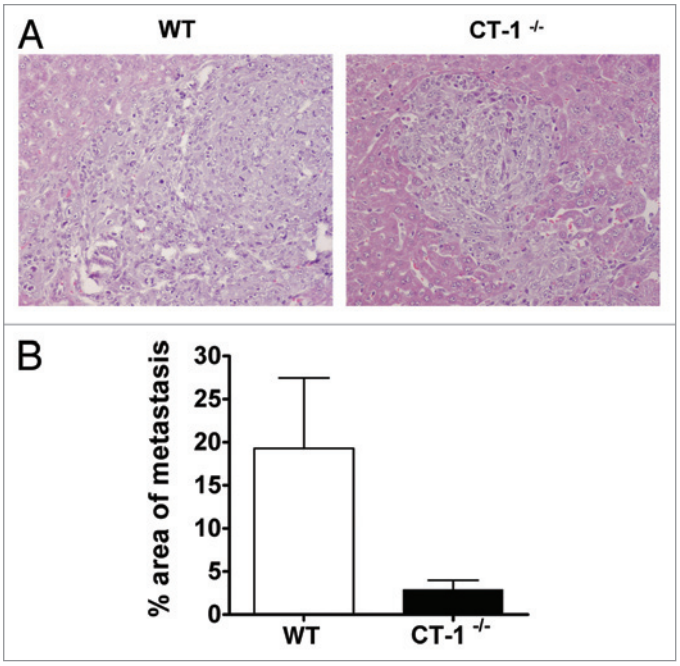

Figure 6. Reduced number of MC38 cell-derived metastases from intrasplenic tumor cell inoculations in *CT-1*$^{-/-}$ mice. (**A**) Representative hematoxylin and eosin (H&E)-stained tissue sections (× 100 magnification) of the liver of wild type (WT) and *CT-1*$^{-/-}$ littermates 14 d after the intrasplenic injection of 5 × 10^6 MC38 cells. (**B**) Percentage of tissue area occupied by tumor nodules was quantified in slides stained with H&E and quantified using the Metamorph software.

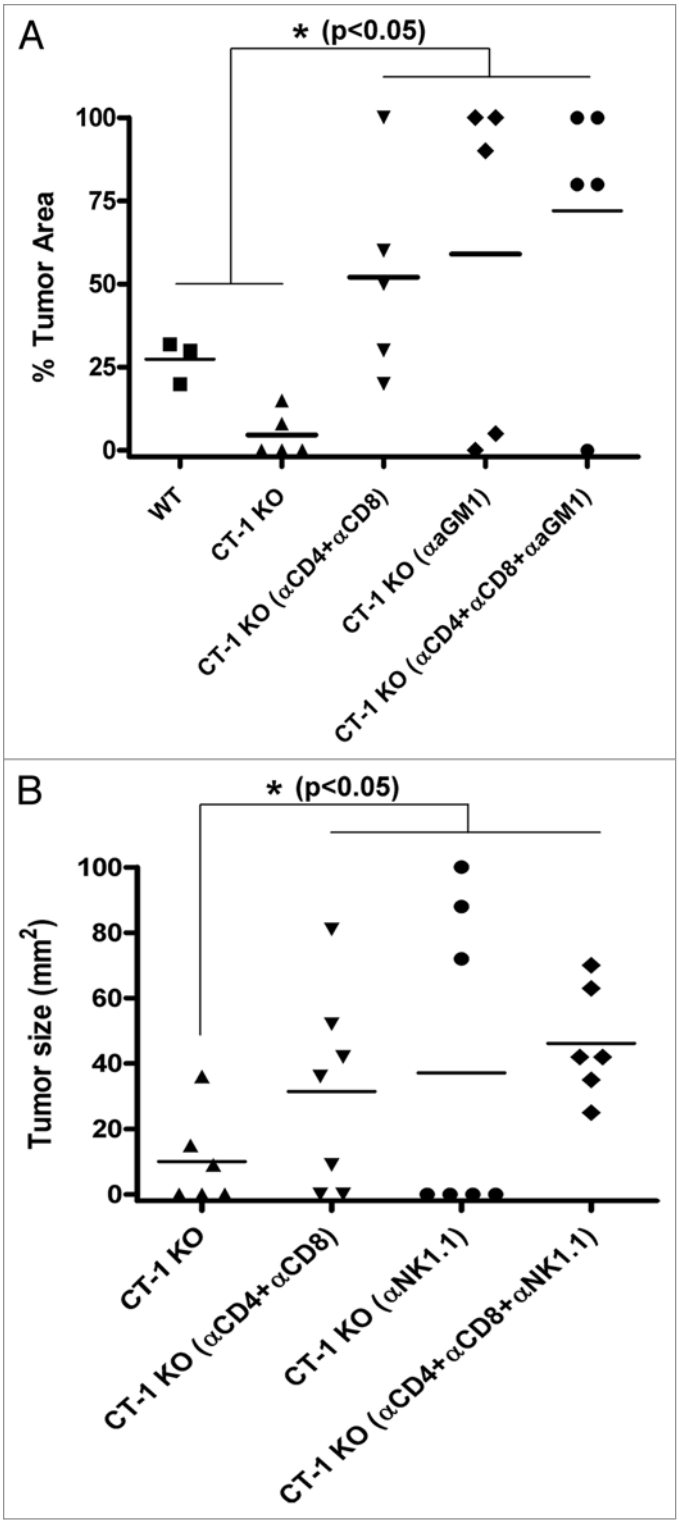

Figure 7 (right). Depletions of T and NK cells restore the engraftment of MC38 tumors in the liver of *CT-1*$^{-/-}$ mice. (**A**) Wild type (WT) and *CT-1*$^{-/-}$ mice were given 5 × 10^6 MC38 cells directly into surgically exposed spleens, as indicated. Mice optionally received a depleting course of anti-CD4 and anti-CD8β antibodies and/or with anti-asialo GM1 antibodies starting 3 d before tumor inoculation. Data represent the individual tumor area in the surface of the liver as assessed 14 d after tumor inoculation. (**B**) Experiments in *CT-1*$^{-/-}$ mice, as those in shown in **Figure 1B** following the intrahepatic injection of MC38 tumor cells. When indicated mice received depleting courses of anti-CD4, anti-CD8β and/or anti-NK1.1 antibodies starting 3 d prior to tumor cell injection. Data represent the individual sizes of hepatic tumors.

leukocytes from WT and *CT-1*$^{-/-}$ mice were used as effector cells. These cells were resuspended in the same medium and placed at various E:T ratios. Labeled target cells were added to each well at a concentration of 3 × 10^3 cells/well for a total volume of 0.2 mL/well. After 5 h incubation, the release of [^{51}Cr] into the supernatant was quantified with a microplate scintillation counter (Packard TopCount, PerkinElmer, C990201). The percentage of cytotoxicity was calculated as the percentage of [^{51}Cr] release using the following equation: (experimental release – spontaneous release) / (maximum release – spontaneous release) × 100.

Surgical inoculation and follow up of tumors. A single cell suspension was prepared in phosphate buffered saline and kept on ice. Mice were anesthetized using inhaled isoflurane (Esteve, 13400264). A small nick was made in the skin and the abdominal wall musculature was grasped and lifted up. The abdominal cavity was accessed and a single blade of the scissors used to push the intra-abdominal contents away. The liver is identified and exposed. A 29 G or fine needle (Hamilton Company, 7637–01) was used to inject a 25 μL volume of cell suspension. Finally, the liver was returned to the abdominal cavity and mouse was sutured. For tumor size studies, mice underwent a second laparotomy or were euthanized for necropsy.

Formalin-fixed, paraffin tissue sections were stained with hematoxylin and eosin (H&E). Quantification of metastasis was performed using a computer-based image analysis system equipped with Metamorph software (Universal Imaging Corp.). Briefly, the images of H&E staining were acquired at × 100 (× 10 ocular and × 20 objective) directly from slides to a computer using a Zeiss (Carl Zeiss, Inc.) microscope.

Proliferation assays. MC38 cells were cultured in 96-well plates in RPMI 1640 medium. Later, [methyl-^{3}H]thymidine uptake was determined by the addition of 1 μCi of [methyl-^{3}H] thymidine (25 Ci mmol^{-1}; GE Healthcare, TRK300–5MCI) for 16–20 h. At the end of the labeling time, [methyl-^{3}H]thymidine uptake was determined by transferring cells to 96-well filter microplates (Unifilter-96 GF/C, PerkinElmer, 6005174) and adding 25 μL of scintillation liquid (Microscint O, PerkinElmer, 6013611) to measure radioactivity.

Isolation of liver leukocytes. Livers from different mice were surgically harvested. Minced liver lobes were incubated in collagenase D (Roche, 1088–866) and DNase I (Roche, 1284–982) for 15 min at 37°C. Dissociated cells were passed through a 70 μm nylon mesh filter (BD Falcon, BD Bioscience, 352350) and washed. Dead cells, debris and hepatocytes were then removed with Percoll gradients (Sigma-Aldrich, P7828). Cells were also treated with ACK lysing buffer (Lonza, 10–548E) to remove residual red cells and washed before further analysis.

Administration of AdCT-1. AdCT-1 and AdLacZ were generated[30] and expanded as previously described.[3] Animals received 1×10^9 plaque-forming units (pfu) of AdCT-1 (n = 12) or AdLacZ (n = 12) in 100 μL PBS intravenously (retro-orbital injection) 48 h before receiving intrahepatic or intrasplenic cell suspensions.

Generation of MAB19. *CT-1*$^{-/-}$ mice were immunized with mouse CT-1 (R&D, 438-CT-050/CF) and hybridomas were produced as described[31] by conventional fusion techniques. Monoclonal antibodies were selected by ELISA and immunoblotting.

Indirect ELISA for screening of monoclonal anti-CT-1. Briefly, high binding microtiter plates (Greiner, M2936–100EA) were coated with CT-1 (1 μg/mL) in 0.06 M carbonate buffer (pH 9.6) and incubated overnight at 4°C. Plates were washed 3 times with PBS-Tween 0.05% (PBS-T) and blocked with PBS plus 0.5% Casein (PBS-CAS) for 2 h at 37°C. Antibody supernatants were added to the wells in duplicate and incubated for 1 h at 37°C. After washing, plates were incubated with Goat IgG anti-mouse IgG antibody labeled with peroxidase (Pierce, 32430), diluted 1:5.000 in PBS-T, for 1 h at 37°C. After washing again the reaction was revealed by adding 0.01 M 2,2'-azino-bis(3-ethylbenzthiazoline-6-sulphonic acid) (ABTS, Roche, A9941) in citrate buffer containing 0.03% H_2O_2, and optical density (OD) was determined at 405 nm. Quality, positive and negative controls were included in each plate. The cut off was established as the mean absorbance values for irrelevant IgG plus three standard deviations.

Immunoblotting assays. CT-1 was separated on 12% SDS-PAGE under reducing conditions, and electrotransferred to 0.2 μm nitrocellulose membranes. Non-specific interactions were blocked by 0.5% casein in PBS incubation, for 2 h at room temperature. Nitrocellulose membrane was then incubated with hybridoma supernatants through a Multiscreen device (Bio-Rad, 170–4017). IgG binding was detected by incubating a secondary antibody, Goat anti-mouse IgG labeled with peroxidase (Pierce), diluted at 1:10.000 in PBS-tween, for 1h at room temperature. Reaction was revealed by adding western Lightning-ECL peroxidase chemiluminescent substrate (Perkin Elmer, NEL111001EA). Preimmune sera and culture media were added as negative controls. A commercial antibody against CT-1 (R&D) was used as positive control.

Statistics. Comparisons were made with paired Student's t-tests and log-rank using Prism software (Graph Pad Software). p values are reported.

Disclosure of Potential Conflicts of Interest

No potential conflicts of interest were disclosed.

Acknowledgments

Elena Ciordia and Eneko Elizalde are acknowledged for excellent animal facility management, as well as technical help by Arantza Azpilikueta. Financial support was from MEC/MICINN (SAF2005–03131 and SAF2008–03294), Departamento de Educación del Gobierno de Navarra, Departamento de Salud del Gobierno de Navarra (Beca Ortiz de Landázuri). Redes temáticas de investigación cooperativa RETIC (RD06/0020/0065), Fondo de investigación sanitaria (FIS PI060932 and PI10/01516), European commission 7th famework program (ENCITE) and SUDOE-IMMUNONET, Fundacion Mutua Madrileña, Programa "Tú eliges: tú decides" de Caja Navarra and "UTE for project FIMA." MS-H receives a Ramon y Cajal contract from Ministerio de Educación y Ciencia. CA is supported by Fundación Científica de la Asociación Española Contra el Cáncer (AECC).

Supplemental Material

Supplemental material may be found here:
www.landesbioscience.com/journals/oncoimmunology/article/22504/

References

1. Pennica D, Wood WI, Chien KR. Cardiotrophin-1: a multifunctional cytokine that signals via LIF receptor-gp 130 dependent pathways. Cytokine Growth Factor Rev 1996; 7:81-91; PMID:8864356; http://dx.doi.org/10.1016/1359-6101(96)00007-X.
2. Silver JS, Hunter CA. gp130 at the nexus of inflammation, autoimmunity, and cancer. J Leukoc Biol 2010; 88:1145-56; PMID:20610800; http://dx.doi.org/10.1189/jlb.0410217.
3. Bustos M, Beraza N, Lasarte JJ, Baixeras E, Alzuguren P, Bordet T, et al. Protection against liver damage by cardiotrophin-1: a hepatocyte survival factor up-regulated in the regenerating liver in rats. Gastroenterology 2003; 125:192-201; PMID:12851883; http://dx.doi.org/10.1016/S0016-5085(03)00698-X.
4. Beraza N, Marqués JM, Martínez-Ansó E, Iñiguez M, Prieto J, Bustos M. Interplay among cardiotrophin-1, prostaglandins, and vascular endothelial growth factor in rat liver regeneration. Hepatology 2005; 41:460-9; PMID:15723445; http://dx.doi.org/10.1002/hep.20590.
5. Marquès JM, Belza I, Holtmann B, Pennica D, Prieto J, Bustos M. Cardiotrophin-1 is an essential factor in the natural defense of the liver against apoptosis. Hepatology 2007; 45:639-48; PMID:17326158; http://dx.doi.org/10.1002/hep.21508.
6. Iñiguez M, Berasain C, Martinez-Ansó E, Bustos M, Fortes P, Pennica D, et al. Cardiotrophin-1 defends the liver against ischemia-reperfusion injury and mediates the protective effect of ischemic preconditioning. J Exp Med 2006; 203:2809-15; PMID:17178916; http://dx.doi.org/10.1084/jem.20061421.

7. Moreno-Aliaga MJ, Pérez-Echarri N, Marcos-Gómez B, Larequi E, Gil-Bea FJ, Viollet B, et al. Cardiotrophin-1 is a key regulator of glucose and lipid metabolism. Cell Metab 2011; 14:242-53; PMID:21803294; http://dx.doi.org/10.1016/j.cmet.2011.05.013.
8. Conze D, Weiss L, Regen PS, Bhushan A, Weaver D, Johnson P, et al. Autocrine production of interleukin 6 causes multidrug resistance in breast cancer cells. Cancer Res 2001; 61:8851-8; PMID:11751408.
9. Yang ZF, Lau CK, Ngai P, Lam SP, Ho DW, Poon RT, et al. Cardiotrophin-1 enhances regeneration of cirrhotic liver remnant after hepatectomy through promotion of angiogenesis and cell proliferation. Liver Int 2008; 28:622-31; PMID:18312290; http://dx.doi.org/10.1111/j.1478-3231.2008.01687.x.
10. Matsui M, Kishida T, Nakano H, Yoshimoto K, Shin-Ya M, Shimada T, et al. Interleukin-27 activates natural killer cells and suppresses NK-resistant head and neck squamous cell carcinoma through inducing antibody-dependent cellular cytotoxicity. Cancer Res 2009; 69:2523-30; PMID:19244121; http://dx.doi.org/10.1158/0008-5472.CAN-08-2793.
11. Gangadhar T, Schilsky RL; Medscape. Molecular markers to individualize adjuvant therapy for colon cancer. Nat Rev Clin Oncol 2010; 7:318-25; PMID:20440283; http://dx.doi.org/10.1038/nrclinonc.2010.62.
12. Masi G, Fornaro L, Caparello C, Falcone A. Liver metastases from colorectal cancer: how to best complement medical treatment with surgical approaches. Future Oncol 2011; 7:1299-323; PMID:22044204; http://dx.doi.org/10.2217/fon.11.108.
13. Fridman WH, Pagès F, Sautès-Fridman C, Galon J. The immune contexture in human tumours: impact on clinical outcome. Nat Rev Cancer 2012; 12:298-306; PMID:22419253; http://dx.doi.org/10.1038/nrc3245.
14. Pagès F, Kirilovsky A, Mlecnik B, Asslaber M, Tosolini M, Bindea G, et al. In situ cytotoxic and memory T cells predict outcome in patients with early-stage colorectal cancer. J Clin Oncol 2009; 27:5944-51; PMID:19858404; http://dx.doi.org/10.1200/JCO.2008.19.6147.
15. Camus M, Tosolini M, Mlecnik B, Pagès F, Kirilovsky A, Berger A, et al. Coordination of intratumoral immune reaction and human colorectal cancer recurrence. Cancer Res 2009; 69:2685-93; PMID:19258510; http://dx.doi.org/10.1158/0008-5472.CAN-08-2654.
16. Langley RR, Fidler IJ. The seed and soil hypothesis revisited--the role of tumor-stroma interactions in metastasis to different organs. Int J Cancer 2011; 128:2527-35; PMID:21365651; http://dx.doi.org/10.1002/ijc.26031.
17. Seymour K, Charnley RM. Evidence that metastasis is less common in cirrhotic than normal liver: a systematic review of post-mortem case-control studies. Br J Surg 1999; 86:1237-42; PMID:10540123; http://dx.doi.org/10.1046/j.1365-2168.1999.01228.x.
18. Uetsuji S, Yamamura M, Yamamichi K, Okuda Y, Takada H, Hioki K. Absence of colorectal cancer metastasis to the cirrhotic liver. Am J Surg 1992; 164:176-7; PMID:1636899; http://dx.doi.org/10.1016/S0002-9610(05)80380-0.
19. Okuno K, Yasutomi M, Kon M, Hatakeyama K, Muto T, Kitajima M, et al. Intrahepatic interleukin-2 with chemotherapy for unresectable liver metastases: a randomized multicenter trial. Hepatogastroenterology 1999; 46:1116-21; PMID:10370677.
20. Montero-Julian FA, Brailly H, Sautès C, Joyeux I, Dorval T, Mosseri V, et al. Characterization of soluble gp130 released by melanoma cell lines: A polyvalent antagonist of cytokines from the interleukin 6 family. Clin Cancer Res 1997; 3:1443-51; PMID:9815830.
21. Rose-John S, Scheller J, Elson G, Jones SA. Interleukin-6 biology is coordinated by membrane-bound and soluble receptors: role in inflammation and cancer. J Leukoc Biol 2006; 80:227-36; PMID:16707558; http://dx.doi.org/10.1189/jlb.1105674.
22. Crispe IN. The liver as a lymphoid organ. Annu Rev Immunol 2009; 27:147-63; PMID:19302037; http://dx.doi.org/10.1146/annurev.immunol.021908.132629.
23. Kortylewski M, Kujawski M, Wang T, Wei S, Zhang S, Pilon-Thomas S, et al. Inhibiting Stat3 signaling in the hematopoietic system elicits multicomponent antitumor immunity. Nat Med 2005; 11:1314-21; PMID:16288283; http://dx.doi.org/10.1038/nm1325.
24. Yu H, Kortylewski M, Pardoll D. Crosstalk between cancer and immune cells: role of STAT3 in the tumour microenvironment. Nat Rev Immunol 2007; 7:41-51; PMID:17186030; http://dx.doi.org/10.1038/nri1995.
25. Hannani D, Sistigu A, Kepp O, Galluzzi L, Kroemer G, Zitvogel L. Prerequisites for the antitumor vaccine-like effect of chemotherapy and radiotherapy. Cancer J 2011; 17:351-8; PMID:21952286; http://dx.doi.org/10.1097/PPO.0b013e3182325d4d.
26. Oppenheim RW, Wiese S, Prevette D, Armanini M, Wang S, Houenou LJ, et al. Cardiotrophin-1, a muscle-derived cytokine, is required for the survival of subpopulations of developing motoneurons. J Neurosci 2001; 21:1283-91; PMID:11160399.
27. Dubrot J, Palazón A, Alfaro C, Azpilikueta A, Ochoa MC, Rouzaut A, et al. Intratumoral injection of interferon-α and systemic delivery of agonist anti-CD137 monoclonal antibodies synergize for immunotherapy. Int J Cancer 2011; 128:105-18; PMID:20309938; http://dx.doi.org/10.1002/ijc.25333.
28. Mazzolini G, Narvaiza I, Martinez-Cruz LA, Arina A, Barajas M, Galofré JC, et al. Pancreatic cancer escape variants that evade immunogene therapy through loss of sensitivity to IFNgamma-induced apoptosis. Gene Ther 2003; 10:1067-78; PMID:12808437; http://dx.doi.org/10.1038/sj.gt.3301957.
29. Quetglas JI, Dubrot J, Bezunartea J, Sanmamed MF, Hervas-Stubbs S, Smerdou C, et al. Immunotherapeutic Synergy Between Anti-CD137 mAb and Intratumoral Administration of a Cytopathic Semliki Forest Virus Encoding IL-12. Mol Ther 2012; 20:1664-75; PMID:22735380; http://dx.doi.org/10.1038/mt.2012.56.
30. Bordet T, Schmalbruch H, Pettmann B, Hagege A, Castelnau-Ptakhine L, Kahn A, et al. Adenoviral cardiotrophin-1 gene transfer protects pmn mice from progressive motor neuronopathy. J Clin Invest 1999; 104:1077-85; PMID:10525046; http://dx.doi.org/10.1172/JCI6265.
31. Melero I, Gabari I, Tirapu I, Arina A, Mazzolini G, Baixeras E, et al. Anti-ICAM-2 monoclonal antibody synergizes with intratumor gene transfer of interleukin-12 inhibiting activation-induced T-cell death. Clin Cancer Res 2003; 9:3546-54; PMID:14506140.